Simple Indicator of Draw Resonance Instability in Melt Spinning Processes

Joo Sung Lee, Hyun Wook Jung, and Jae Chun Hyun
Dept. of Chemical and Biological Engineering, Applied Rheology Center, Korea University, Seoul 136-701, Korea

L. E. Scriven
Dept. of Chemical Engineering and Materials Science, University of Minnesota, Minneapolis, MN 55455

DOI 10.1002/aic.10498
Published online July 18, 2005 in Wiley InterScience (www.interscience.wiley.com).

Keywords: draw resonance, eigenfunctions, kinematic waves, indicator, traveling times, viscoelastic spinning

Introduction

Draw resonance, one of major instabilities in polymer extensional processes such as fiber spinning and film casting, sets in as the drawdown ratio — the ratio of take-up velocity to extrusion velocity — is raised past its critical value. It appears as sustained periodic variations in velocity, mass-flux, cross-section, and spinline tension. There have been many experimental observations and theoretical analyses of this phenomenon during the four decades.[1-12] However, there are still unsettled issues about draw resonance, many of them expounded by Petrie.[13]

In fiber spinning of Newtonian or viscoelastic liquids, the onset of draw resonance is an oscillatory instability or overstability, as termed by Eddington,[14] or a stable supercritical Hopf bifurcation, as used in the singularity theory. In an analysis by means of the method of infinitesimal disturbances — linear stability analysis — Schultz et al.[6] showed that as the drawdown ratio is raised just beyond the Hopf bifurcation, the frequency of oscillation falls, and, thus, the period of the nascent limit cycle grows. To go beyond linear stability theory and find the nonlinear transient behavior at higher drawdown ratios, some researchers[6, 15, 16] solved nonlinear initial value problems with selected initial conditions and found that the solutions at supercritical drawdown ratios approach stable periodic states, or limit cycles.

To clarify the physics of the occurrence of the bifurcation and persistence of the supercritical oscillating behavior, Hyun and coworkers[5,15-17] focused on kinematic waves that can be envisioned traveling along the spinline. From solutions of the nonlinear transient equations that govern oscillations of a spinline, they identified a combination of three kinds of kinematic waves (waves of spinline throughput, maximum spinline cross-section, and minimum cross-section), and period of oscillation of the spinline, passing through zero at the critical drawdown ratio and, therefore, being an index to the instability. This property of the combination follows from the dominant eigenfunctions, or normal modes, of infinitesimal disturbances at each value of the drawdown ratio, as is established below. Thus, the transition of a spinline from steady to oscillatory behavior as drawdown ratio is raised is a case of well-understood transformation of a stable state to an unstable one and concomitant appearance of a stable limit cycle as a parameter is varied — a stable supercritical Hopf bifurcation.

Equations of Spinline Flow

In the well-established approximation by one-dimensional (1-D) flow the dependent variables are axial velocity v, cross-sectional area a, axial extra stress $\tilde{\tau}$, and the independent variables are time $\tilde{t}$, and spinline distance $\tilde{x}$. The parameters in this system are the zero-shear-rate viscosity, η_0, fluid relaxation time, λ, Deborah number De, drawdown ratio r, and two parameters of PTT fluids ε and ξ.[18] The dimensionless governing equations that describe isothermal spinning of viscoelastic PTT fluids are as follows (Subscripts 0 and L denote the spinneret and takeup conditions, respectively.)

Correspondence concerning this article should be addressed to H. W. Jung at hwjung@grtrkr.korea.ac.kr.

Continuity equation

$$\frac{\partial A}{\partial t} + \frac{\partial}{\partial x}(AV) = 0 \tag{1}$$

where

$$A \equiv \frac{a}{a_0}, \quad V \equiv \frac{v}{v_0}, \quad t \equiv \frac{\tilde{t} v_0}{L}, \quad x \equiv \frac{\tilde{x}}{L}$$

Axial momentum equation

$$\frac{\partial}{\partial x}(A\tau) = 0 \tag{2}$$

where

$$\tau \equiv \frac{\tilde{\tau} L}{2\eta_0 v_0}$$

Constitutive equation: (Phan-Thien and Tanner fluids)

$$K\tau + \mathrm{De}\left(\frac{\partial \tau}{\partial t} + V\frac{\partial \tau}{\partial x} - 2(1-\xi)\tau\frac{\partial V}{\partial x}\right) = \frac{\partial V}{\partial x} \tag{3}$$

where

$$\mathrm{De} \equiv \frac{\lambda_0 v_0}{L}, \quad K \equiv \exp(2\varepsilon\, \mathrm{De}\, \tau)$$

These dimensionless equations are subject to the following boundary conditions

$$A = 1,\ V = 1 \text{ at } x = 0, \quad V = r \text{ at } x = 1,\ t \geq 0 \tag{4}$$

where r is the drawdown ratio $r \equiv v_L/v_0$. Actually, $x = 0$ is taken as the position of maximum extrudate swell near the die exit, in order to exclude the prehistory effect inside the die. The equation system neglects radial extra stress and omits all secondary forces in Eq. 2: gravity, air drag, surface tension, and inertia. Including them would not change the fundamental aspects of what is reported here.

Solutions of the Equations

The earlier equations are readily solved, as described elsewhere.[12, 16] When the drawdown ratio r is smaller than the critical value r_c, all disturbances that can be imposed die out in time. When r is slightly greater, but almost equal to r_c, all disturbances eventually evolve to a tiny, virtually circular limit cycle and periodic solution is essentially sinusoidal. When r is appreciably greater than r_c, all disturbances soon evolve to a distinctly nonlinear limit cycle characteristic of the steady, nonsinusoidal oscillations of established draw resonance as displayed in Figure 1. Although the critical drawdown ratio r_c can be closely estimated from solutions of initial value problems, a far more efficient way of calculating it is to solve the succession of eigenproblems that give the response of flow states at a sequence of drawdown ratios to all possible infinitesimal initial disturbances; that is, to solve the equations of linear stability theory.[3,4,12]

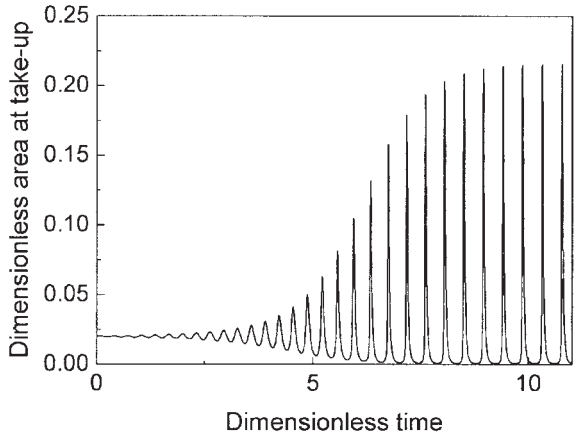

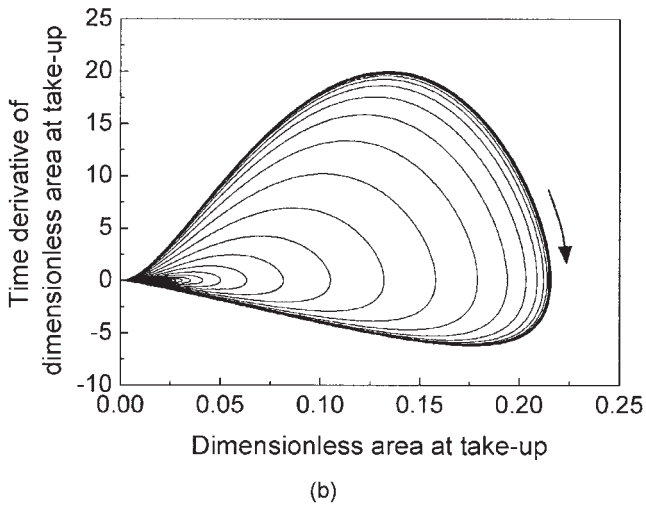

Figure 1. Transient response of spinline cross-sectional area at the take-up of a PTT fluid when $\varepsilon = 0$, $\xi = 0.2$, De = 0.01, and r = 50: (a) temporal picture, and (b) phase plane trajectory.

Stability of Steady Flow States

In short, the linear stability analysis amounts to introducing perturbed variables of the form

$$A(x,t) = A_s(x)[1 + \alpha(x)\exp(\Omega t)],$$
$$V(x,t) = V_s(x)[1 + \beta(x)\exp(\Omega t)],$$
$$\tau(x,t) = \tau_s(x)[1 + \gamma(x)\exp(\Omega t)] \tag{5}$$

in the governing Eqs. 1 $\sim$ 3; noting that terms involving steady-state variables $A_s(x)$, $V_s(x)$, and $\tau_s(x)$ collectively cancelled out; retaining terms linear in the small perturbations $\alpha(x)$, $\beta(x)$, $\gamma(x)$; restricting the class of perturbations by setting boundary conditions on $\alpha(x)$ and $\beta(x)$; and solving for eigen-

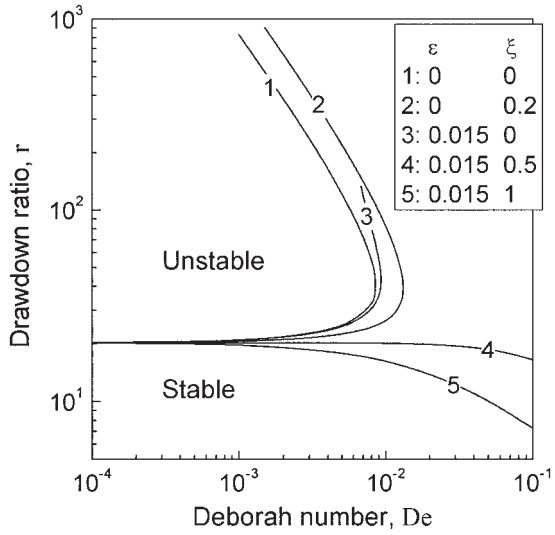

Figure 2. Neutral stability curves of PTT fluids depending on material parameters, ε and ξ.

functions $\{\alpha_n(x),\ \beta_n(x),\ \gamma_n(x)\}$ and eigenvalues Ω_n. The linearized versions of Eqs. 1 ~ 3 are compactly represented in a matrix-vector form

$$\Omega\ \underline{\underline{M}}\,\underline{y} = \underline{\underline{J}}\,\underline{y} \tag{6}$$

where $\underline{y}$ represents a vector of eigenfunctions of α, β, and γ and $\underline{\underline{J}}$, $\underline{\underline{M}}$ are Jacobian and Mass matrices, respectively. Boundary conditions adopted here are that neither cross-sectional area nor velocity are perturbed at $x = 0$, that is, $\alpha(0) = 0$, $\beta(0) = 0$; and that take-up velocity remains unperturbed, that is, $\beta(1) = 0$. The above eigenproblem has been solved using a finite difference scheme and a shift-invert transformation method.

The eigenvalue possessing the largest real part among the eigenpairs $\{\Omega_n, \underline{y}_n\}$ determines the stability of the steady flow state, indicating that the positive real part makes the state unstable. The corresponding imaginary part gives the frequency of sinusoidal oscillation, if any, of the exponentially growing or decaying perturbation. At the critical drawdown ratio r_c, the spinline is marginally stable and the imaginary part gives the frequency, period, and wave speed of infinitesimal sinusoidal waves described by the corresponding eigenfunction, which represents a new flow state. The path of states as r rises splits at r_c in what is called a Hopf bifurcation.[6,19]

Results and Discussion

In the simple Newtonian spinning, the critical drawdown ratio (r_c) and period of oscillation (T) at this point are readily predicted, that is, $r_c = 20.218$, $T = 0.4484$. Also, neutral stability curves of viscoelastic PTT fluids depending on Deborah number and parameters, ε and ξ, are portrayed in Figure 2. It is noted here that in the PTT case, the initial stress at die exit as an unknown should be carefully selected to evaluate the steady states and its stability below unattainable solution regime, especially in the case of $\xi > 0.5$.[20] So, examining the stability diagrams in detail, we can discern the way changes in particular process conditions influence the stability, that is, stabilize or destabilize. However, there still remains the fundamental question: the physics behind the phenomenon as to why such instability arises is not clear.

In an effort to answer this question, the behavior of the various kinematic waves traveling on the spinline from the spinneret to the take-up has been examined by Hyun and coworkers.[5,15-17] That is, from the periodic solutions or limit cycles obtained by the nonlinear transient simulations of spinning systems, the speeds and traveling times of several kinematic waves have been predicted.[15,16] And, it has been revealed that among the many kinds of kinematic waves propagating on the spinline, maximum and minimum cross-section waves (A_{max} and A_{min}), and unity-throughput (AV) waves, which travel the entire spinline, satisfy a certain relationship and play a key role to determine the draw resonance. The stability criterion or indicator for draw resonance was devised, comparing the traveling times of these waves as Eq. 7

$$(t_L)_1 + (t_L)_2 + \frac{T}{2} \begin{matrix} > \\ < \end{matrix} (\theta_L)_1 + (\theta_L)_2 \quad \text{for } r \begin{matrix} < \\ > \end{matrix} r_c \tag{7}$$

where $(t_L)_1$ and $(t_L)_2$ represent dimensionless traveling times of two consecutive unity-throughput waves from the spinneret to the take-up, T is dimensionless period of oscillation, $(\theta_L)_1$ and $(\theta_L)_2$ are dimensionless traveling times of maximum and minimum cross-sectional area waves from node 1 to the take-up, respectively. These traveling times, t_L and θ_L are defined as follows

$$\theta_L = \int_{x_1}^{1} \frac{dx}{W}, \quad \text{where } W = \left(\frac{\partial x}{\partial t}\right)_{A_{max}} \text{ or } \left(\frac{\partial x}{\partial t}\right)_{A_{min}} \tag{8}$$

$$t_L = \int_{0}^{1} \frac{dx}{U}, \quad \text{where } U = \left(\frac{\partial x}{\partial t}\right)_{AV=1} \tag{9}$$

where W and U are traveling speed of A_{max} (or A_{min}) waves and unity-AV waves, respectively.

As will be fully explained next, it has been found that the indicator relationship for draw resonance, Eq. 7 can be exactly and more easily estimated from the dominant eigenfunctions, or normal modes of linear system.

A set of dominant eigenfunctions of spinline cross-section and velocity obtained from the linear stability[6] will be used to evaluate the characteristics of traveling waves, such as their traveling speeds and times, portraying the transient behavior of spinline variables of Eq. 5. The transient solutions given by the dominant eigenfunction or normal mode conserving mass and momentum and satisfying the end conditions have proved periodically stable at drawdown ratio larger than its critical value, whereas steady-state solutions are not stable, that is, a supercritical Hopf bifurcation. That is why steady-state spinning gives rise to persistent draw resonance at higher drawdown ratio.

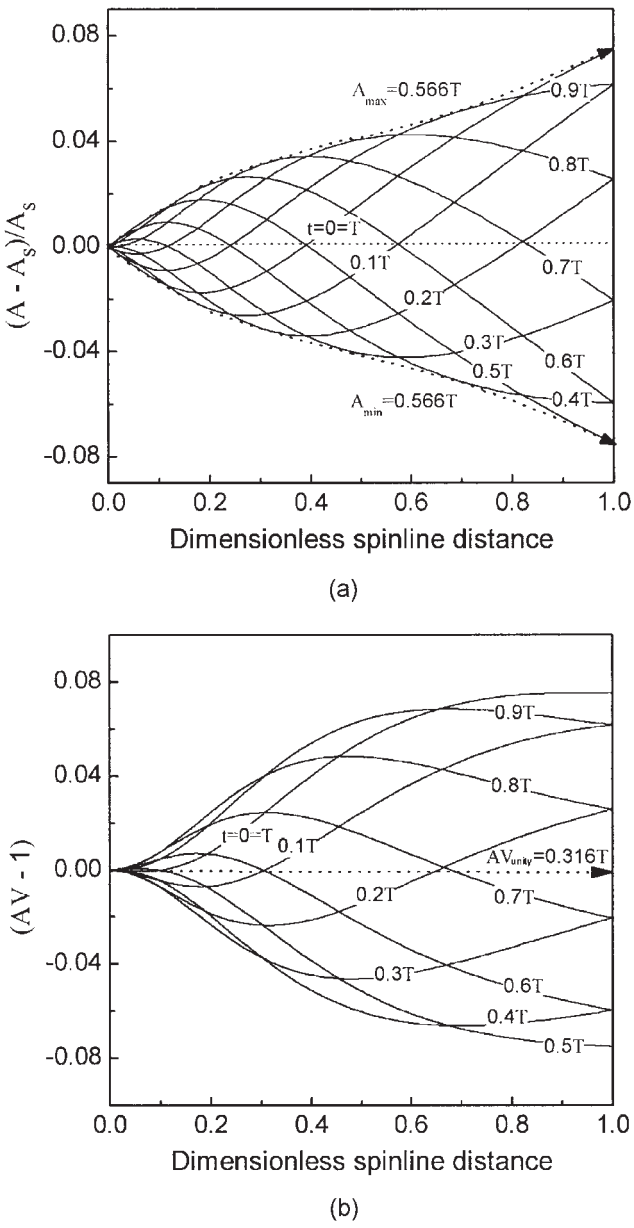

Figure 3. Transient solutions of (a) the perturbed cross-sectional area, and (b) the perturbed throughput during one period of oscillation at the onset of Newtonian spinning.

Figure 3 shows families of cross-section and throughput curves at the onset during one period of oscillation at the onset of Newtonian case. Local features of the dominant eigenfunction propagate along the flow at speeds given by the dominant eigenvalue. For a Newtonian case, the traveling times from the spinneret to take-up of maxima or minima in cross-section vs. time are 0.566 of the period of oscillation; that of unity-throughput is 0.316 of the period, exactly satisfying the relationship of the indicator, Eq. 7. Therefore, a combination of the period of oscillation and three kinematic waves indeed passes through zero when the drawdown ratio is at the critical value for marginal stability and bifurcation.

Solving the eigenproblems is much faster and easier than solving the nonlinear systems, because the traveling speeds (W and U) and times (θ_L and t_L) of aforementioned waves can be directly determined from eigenfunction data without further transient computations. For example, the successive times of $A_{\max}$ or $A_{\min}$ at each fixed spinline location can be analytically predicted using the relationship, $[\partial(\Re(A))/\partial t]_x = 0$.

$$f \equiv [\partial(\Re(A))/\partial t]_x = (\alpha_R\Omega_R - \alpha_I\Omega_I)\cos(\Omega_I\theta_j^*) - (\alpha_I\Omega_R + \alpha_R\Omega_I)\sin(\Omega_I\theta_j^*) = C\cos(\Omega_I\theta_j^*) - D\sin(\Omega_I\theta_j^*) = 0 \quad (10)$$

where $\Re$ denotes the real part of a function, θ_j^* is times for $A_{\max}$ (or $A_{\min}$) at the fixed location j, α_R and α_I are real and imaginary parts of dominant eigenfunctions of cross-sectional perturbation, respectively. Once above data are known, traveling times of $A_{\max}$ (or $A_{\min}$) can be simply evaluated by Eq. 8 and the following expression of their speed, W of Eq. 11

$$W = \left(\frac{\partial x}{\partial t}\right)_f = -\frac{\left(\frac{\partial f}{\partial t}\right)_x}{\left(\frac{\partial f}{\partial x}\right)_t} = \frac{\lambda_I C\sin(\Omega_I\theta_j^*) + \lambda_I D\cos(\Omega_I\theta_j^*)}{\left(\Omega_R\frac{\partial\alpha_R}{\partial x} - \Omega_I\frac{\partial\alpha_I}{\partial x}\right)\cos(\Omega_I\theta_j^*) - \left(\Omega_R\frac{\partial\alpha_I}{\partial x} + \Omega_I\frac{\partial\alpha_R}{\partial x}\right)\sin(\Omega_I\theta_j^*)} \quad (11)$$

In the similar way, times for unity-throughput waves at each fixed location, which are used for the evaluation of traveling times t_L (Eq. 9), and their speed U (Eq. 13), can be analytically determined

$$g \equiv \Re(AV - 1) = \delta_R\cos(\Omega_I t_j^*) - \delta_I\sin(\Omega_I t_j^*) = 0 \quad (12)$$

where $\delta_R = \alpha_R + \beta_R$, $\delta_I = \alpha_I + \beta_I$

$$U = \left(\frac{\partial x}{\partial t}\right)_g = -\frac{\left(\frac{\partial g}{\partial t}\right)_x}{\left(\frac{\partial g}{\partial x}\right)_t} = \frac{\Omega_I\delta_R\sin(\Omega_I t_j^*) + \Omega_I\delta_I\cos(\Omega_I t_j^*)}{\left(\frac{\partial\delta_R}{\partial x}\right)\cos(\Omega_I t_j^*) - \left(\frac{\partial\delta_I}{\partial x}\right)\sin(\Omega_I t_j^*)} \quad (13)$$

These velocities of unity-AV waves, as well as $A_{\max}$ or $A_{\min}$ waves at the onset point from above equations exactly correspond with Figure 1 in Jung et al.[17]

Results by nonlinear and linear analyses as to the indicator equation, Eq. 7 are compared in Figure 4a and b. Traveling times by three kinds of waves and the period from both analyses are plotted against the drawdown ratio r, exhibiting that the magnitudes of the both sides of Eq. 7 change as the drawdown ratio increases beyond its onset value r_c. In the unstable region, the values of traveling times and period esti-

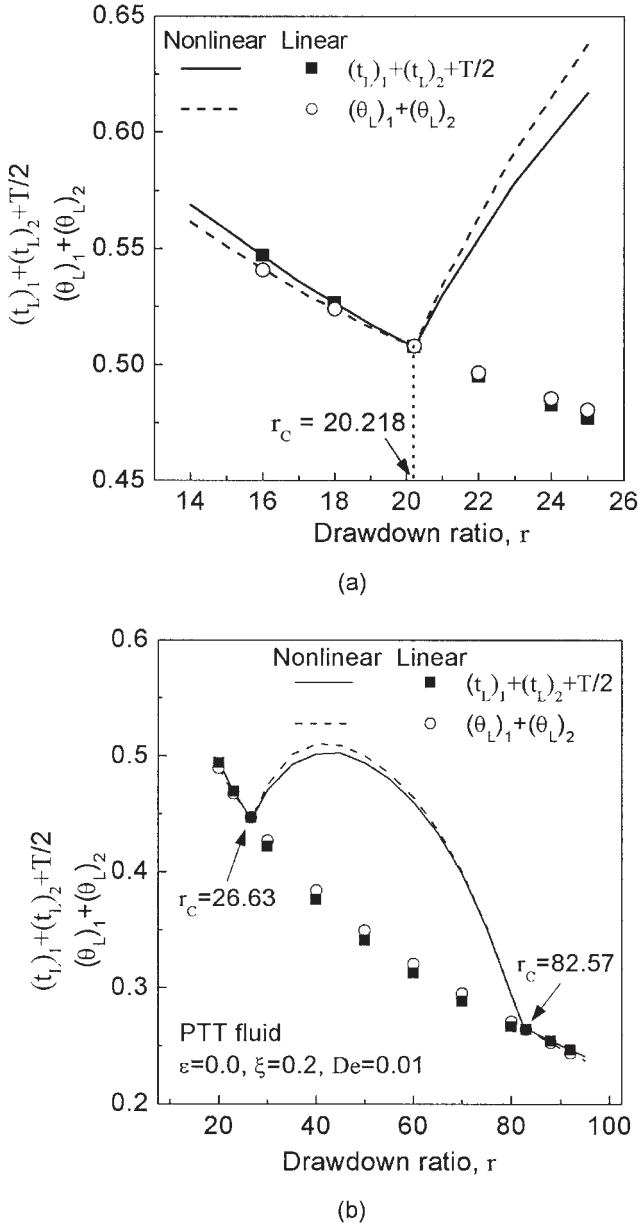

Figure 4. Determination of the stability by the indicator relationship, Eq. 7, for (a) Newtonian, and (b) PTT fluids in both linear (symbols) and nonlinear (lines) cases.

mated from both methods are theoretically different from each other due to the limitations of the linear analysis incapable of portraying nonlinear behavior of limit cycles. Figure 4b compares the results of indicator equation in the viscoelastic PTT case. Even though the values of indicator equation by linear analysis are not in accord with those by nonlinear analysis in the unstable region, these values correctly predict two onset points and demarcate the stable and unstable regions.

It has, thus, been confirmed that the indicator for draw resonance instability explains the results by both linear and nonlinear analyses. Also, as an easy method to elucidate the draw resonance and analyze the kinematic waves traveling the spinline, eigenfunctions or normal modes of the linearized system can be readily applied to more complicated spinning system including cooling, and crystallization kinetics, or other extensional deformation processes.

Conclusions

The draw resonance phenomenon, long known to govern the onset of instability occurring in the polymer processes, has been investigated using the eigenfunction data from the generalized eigenproblem for the Newtonian and viscoelastic spinning. The eigenmodes of the linearized system have been analyzed to reveal the local features of the dominant eigenfunction, in the form of kinematic waves, to propagate along the flow at speeds given by the dominant eigenvalue. As with the draw resonance previously studied with the nonlinear transient simulations,[15,16] a combination of the period of oscillation and the traveling times of zero perturbation of the throughput, and of the maximum and minimum cross-sectional areas evaluated from the eigenfunction data satisfied the same stability criterion illustrating the general stability and bifurcation phenomena of the system. It has been proved that solving the generalized eigenproblems is superior to solving a sequence of transient flow problems and evaluating traveling times of features viewed as kinematic waves.

Acknowledgments

This study was supported by the research grants from 3M company, and the Korea Science and Engineering Foundation (KOSEF) through the Applied Rheology Center (ARC), Seoul, Korea.

Literature Cited

1. Kase S, Matsuo T. Studies on melt spinning. I. Fundamental equations on the dynamics of melt spinning. *J of Polymer Sci. Part A*. 1965;3: 2541-2554.
2. Pearson JRA, Matovich MA. Spinning a molten threadline: stability. *Ind and Eng Chem Fundamentals*. 1969;8:605-609.
3. Gelder D. The stability of fiber drawing processes. *Ind and Eng Chem Fundamentals*. 1971;10:534-535.
4. Fisher RJ, Denn MM. A theory of isothermal melt spinning and draw resonance. *AIChE J*. 1976;22:236-246.
5. Hyun JC. Theory of draw resonance: I. Newtonian fluids. *AIChE J*. 1978;24:418-422, also, Part II. Power-law and Maxwell fluids. 1978; 24:423-426.
6. Schultz WW, Zebib A, Davis SH, Lee Y. Nonlinear stability of Newtonian fibres. *J of Fluid Mechanics*. 1984;149:455-475.
7. Liu B, Beris AN. Time-dependent fiber spinning equations. 2. Analysis of the stability of numerical approximations. *J of Non-Newtonian Fluid Mechanics*. 1988;26:363-394.
8. Anturkar NR, Co A. Draw resonance in film casting of viscoelastic fluids: a linear stability analysis. *J of Non-Newtonian Fluid Mechanics*. 1988;28:287-307.
9. Lee WS, Park CW. Stability of a bicomponent fiber spinning flow. *J of Applied Mechanics*. 1995;62:511-516.
10. Van der Hout R. Draw resonance in isothermal fibre spinning of Newtonian and power-law fluids. *Euro J of Applied Maths*. 2000;11: 129-136.
11. Lee JS, Jung HW, Hyun JC. Frequency response of film casting process. *Korea-Australia Rheology J*. 2003;15:91-96.
12. Jung HW, Lee JS, Scriven LE, Hyun JC. The sensitivity and stability of spinning process using frequency response method. *K J of Chem Eng*. 2004;21:20-26.
13. Petrie CJS. Some remarks on the stability of extensional flows. *Progress and Trends in Rheology*. 1988;II:9-14.
14. Drazin PG, Reid WH. Hydrodynamic stability. Cambridge: Cambridge University Press; 1981.
15. Kim BM, Hyun JC. Oh JS, Lee SJ. Kinematic waves in the

isothermal melt spinning of Newtonian fluids. *AIChE J*. 1996;42: 3164-3169.
16. Jung HW, Song HS, Hyun JC. Draw resonance and kinematic waves in viscoelastic isothermal spinning. *AIChE J*. 2000;46:2106-2111.
17. Jung HW, Choi SM, Hyun JC. Approximate method for determining the stability of the film-casting process. *AIChE J*. 1999;45: 1157-1160.
18. Phan-Thien N. A nonlinear network viscoelastic model. *J of Rheology*. 1978;22:259-283.
19. Demay Y. Instabilité d'étirage et bifurcation de Hopf. France: L'Université de Nice; 1983. PhD.
20. Petrie CJS. *Elongational flows*, London: Pitman, 1979.

Manuscript received July 20, 2004, and revision received Dec. 26, 2004.